bioRxiv preprint doi: https://doi.org/10.1101/2020.01.14.905745; this version posted January 15, 2020. The copyright holder for this preprint (which was not certified by peer review) is the author/funder. All rights reserved. No reuse allowed without permission.

A mitochondria-targeted antioxidant and a thyroid hormone affect carotenoid ketolase gene expression and bill redness in zebra finches

Alejandro Cantarero[1,2], Pedro Andrade[3], Miguel Carneiro[3], Adrián Moreno-Borrallo[2] and Carlos Alonso-Alvarez[2*]

AC ORCID: 0000-0002-5816-701X; PA: 0000-0003-2540-2471; MC: 0000-0001-9882-7775; CAA: 0000-0002-4765-551X

[1] Section of Ecology, Department of Biology, University of Turku, Turku 20014, Finland.

[2] Departamento de Ecología Evolutiva. Museo Nacional de Ciencias Naturales - CSIC. C/ José Gutiérrez Abascal 2, 28006 Madrid, Spain

[3] CIBIO/InBIO, Centro de Investigação em Biodiversidade e Recursos Genéticos, Campus Agrário de Vairão, Universidade do Porto, 4485-661, Vairão, Portugal.

Author contributions: AC, MC and PC, AMB, CAA

AC and CAA designed the study, carried out the experiment and analysed data;

CAA led the writing of the manuscript;

MC, PC and AMB were involved in laboratory analyses;

Data will be publicly available at https://digital.csic.es when finally accepted.

*Corresponding author, email: carlos.alonso@csic.es

Telephone number: +34 91 411 13 28 – 988978

Acknowledgements

bioRxiv preprint doi: https://doi.org/10.1101/2020.01.14.905745; this version posted January 15, 2020. The copyright holder for this preprint (which was not certified by peer review) is the author/funder. All rights reserved. No reuse allowed without permission.

We thank Luisa Amo for providing us with some of the birds in the experiment and Lucía Arregui and Diego Gil for assistance in thyroid hormone quantification. Financial support was obtained from the project CGL2015-69338-C2-2-P (MINECO). AC is currently supported by a postdoctoral fellowship from Fundación Ramón Areces. The experiment was approved by the Bioethics Committee of CSIC and Junta de Castilla La Mancha (JCCM) government (ref number 16-2017).

bioRxiv preprint doi: https://doi.org/10.1101/2020.01.14.905745; this version posted January 15, 2020. The copyright holder for this preprint (which was not certified by peer review) is the author/funder. All rights reserved. No reuse allowed without permission.

ABSTRACT

Conspicuous ornaments in animals can evolve to reveal individual quality when their production/maintenance costs make them reliable as signals or if their expression level is intrinsically linked to quality by some unfalsifiable mechanism (quality indices). The latter has been mostly associated with traits constrained by body size. However, red ketocarotenoid-based coloured ornaments may also have evolved as quality indices because their production could be closely linked to individual metabolism and, particularly, to the cell respiration at the inner mitochondrial membrane (IMM). This mechanism would supposedly not depend on resource (yellow carotenoids) availability, thus discarding allocation trade-offs. A gene coding for a ketolase enzyme (CYP2J19) responsible for converting dietary yellow carotenoids to red ketocarotenoids has recently been described in birds. It is not known, however, if this ketolase is involved in mitochondrial metabolism and if its expression level and activity is resource independent. Here, we manipulated the metabolism of captive male zebra finches by an antioxidant designed to penetrate the IMM (mitoTEMPO) and a thyroid hormone (triiodothyronine; T3) with known hypermetabolic effects. The expression levels of a ketocarotenoid-based ornament (bill redness) and *CYP2J19* were measured. MitoTEMPO downregulated *CYP2J19* expression, supporting the mitochondrial involvement in ketolase function. T3 also reduced *CYP2J19* expression, but at an intermediate dosage, this effect being buffered by mitoTEMPO. Bill redness seemed to show a similar interacting effect. Nevertheless, this faded when *CYP2J19* expression level was controlled for as a covariate. We argue that the well-known mitoTEMPO effect in reducing mitochondrial reactive oxygen species (ROS) production (particularly superoxide) could have interfered on redox signalling mechanisms controlling ketolase transcription. High T3 levels, contrarily, can lead to high ROS production but also trigger compensatory mechanisms,

bioRxiv preprint doi: https://doi.org/10.1101/2020.01.14.905745; this version posted January 15, 2020. The copyright holder for this preprint (which was not certified by peer review) is the author/funder. All rights reserved. No reuse allowed without permission.

which may explain the U-shaped effect with dosage on *CYP2J19* expression levels. Bill *CYP2J19* expression values were also positively correlated to redness and circulating substrate carotenoid levels. Nonetheless, treatment effects did not change when controlling for blood carotenoid concentration, suggesting that resource-availability dependence was irrelevant. Finally, our findings reveal a role for thyroid hormones in the expression of carotenoid-based ornaments that has virtually been ignored until now.

Keywords: cell metabolism, electron transport chain, mito-targeted antioxidants, oxidative stress, red colourations, sexual selection, sexual signalling, *Taeniopygia guttata*.

bioRxiv preprint doi: https://doi.org/10.1101/2020.01.14.905745; this version posted January 15, 2020. The copyright holder for this preprint (which was not certified by peer review) is the author/funder. All rights reserved. No reuse allowed without permission.

Introduction

The animal signalling theory proposes that traits involved in animal communication, such as many conspicuous ornaments and songs, evolve (1) due to production/maintenance costs that prevent cheating by low-quality individuals (Grafen 1990) or (2) because the level of expression of the trait directly reveals individual quality (i.e. they cannot be faked; Maynard Smith & Harper 2003). The first type of trait has often been defined as "signals" (or "handicap signals"), whereas the second type of trait has been defined as "indices" (e.g. Johnstone 1995; Weaver, Koch & Hill 2017). The expression level of sexual "signals" should in some way correlate positively with reproductive success, but negatively to survival, due to some direct or indirect costs of trait production/maintenance. Instead, an "index" should positively correlate to both reproductive success and survival (i.e. no trade-off should exist; Vanhooydonck *et al.* 2007) and is supposedly cost-free (but see Biernaskie, Grafen & Perry 2014). Most examples of indices have been associated with traits (e.g. deer antlers or calling rates) that depend or are positively correlated to body size (Maynard Smith & Harper 2003; Reby & McComb 2003).

However, a new quite different type of index has been proposed in the form of conspicuous colourations produced by red carotenoid pigments (Hill 2011; Weaver *et al.* 2017). Red carotenoid-based ornaments are present in many vertebrates. They have attracted much attention from evolutionary ecologists as its proximate production mechanisms are intriguingly complex (e.g. McGraw 2006). Such complexity is, however, becoming to be disentangled (e.g. Johnson & Hill 2013; Lopes *et al.* 2016; Mundy *et al.* 2016), providing material to propose new evolutionary hypotheses in the signalling theory framework (Hill 2011). The underlying question is why these mechanisms have promoted the selection of red ornaments as reliable information transmitters.

bioRxiv preprint doi: https://doi.org/10.1101/2020.01.14.905745; this version posted January 15, 2020. The copyright holder for this preprint (which was not certified by peer review) is the author/funder. All rights reserved. No reuse allowed without permission.

Carotenoids are molecules whose chromophore generates yellow to red colourations (Britton 2008). The animal organism cannot synthesize them from any non-carotenoid substrate, but some carotenoids can be transformed into others by enzymatic reactions (Stradi *et al.* 1997; McGraw 2006; García-de Blas, Mateo & Alonso-Alvarez 2016). This is the case of red ketocarotenoids (e.g. astaxanthin, canthaxanthin) obtained from dietary yellow-to-orange carotenoids (e.g. lutein, zeaxanthin). This mechanism has been well studied in birds (McGraw 2006). Many aquatic bird species can easily obtain red ketocarotenoids from their food and directly allocate them to ornaments without transformation because ketocarotenoids are abundant in aquatic invertebrate prey (e.g. crustaceans; McGraw 2006). However, among terrestrial birds, ketocarotenoids are often scarce in food (particularly in vegetal food) and molecular mechanisms allowing to transform yellow to red pigments have evolved (McGraw 2006). Currently, the only candidate gene implicated in this transformation and well-supported by molecular studies is *CYP2J19* (Lopes *et al.* 2016; Mundy *et al.* 2016; Twyman *et al.* 2016; 2018). This is a member of the cytochrome p450 family of enzymes, most of its members being involved in the metabolism of toxicants but also in hormone synthesis (Tompkins & Wallace 2007).

Before the discovery of *CYP2J19*, some researchers argued that the candidate enzyme should be linked to mitochondrial activity (Hill 2011; Johnson & Hill 2013). They argued that the molecular similarity between some ketocarotenoids and ubiquinone, which is a key antioxidant involved in the cell respiratory chain, implies that the enzyme could be part of the ubiquinone enzymatic biosynthesis pathway (Johnson & Hill 2013). The transformation would, hence, be made in the inner mitochondrial membrane (IMM) probably sharing a biochemical pathway with cell respiration. The theoretical link to the mitochondria metabolism led these authors (see Hill 2011; Hill & Johnson 2012) to

bioRxiv preprint doi: https://doi.org/10.1101/2020.01.14.905745; this version posted January 15, 2020. The copyright holder for this preprint (which was not certified by peer review) is the author/funder. All rights reserved. No reuse allowed without permission.

propose that red ketocarotenoid based ornaments evolved as "indices" of individual quality as they would be tightly linked to basic metabolic pathways such as cell respiration.

The subsequent description of *CYP2J19* could support this hypothesis if the enzyme is indeed placed at the IMM affecting cell respiration. The recent finding of relatively high levels of ketocarotenoids at the IMM compared to other cell fractions is consistent with this scenario (Hill *et al.* 2019). Moreover, the treatment of male zebra finches (*Taeniopygia guttata*) with a synthetic ubiquinone (mitoQ; Smith *et al.* 2003) designed to penetrate into the IMM has been shown to increase bill redness (Cantarero & Alonso-Alvarez 2017), which is a ketocarotenoid-based sexually selected ornament (McGraw & Toomey 2010).

In the present study, we exposed male zebra finches to another synthetic mito-targeted antioxidant, testing, for the first time, potential changes in bill *CYP2J19* expression levels. This experiment allows us to infer if mitochondria metabolism is indeed linked to the candidate gene and if that connection affects trait expression (redness). The antioxidant (i.e. mitoTEMPO: (2-(2,2,6,6-Tetramethylpiperidin-1-oxyl-4-ylamino)-2-oxoethyl)triphenylphosphonium chloride; Dikalova *et al.* 2010) is similar to mitoQ. In both molecules, the antioxidant is joined to a triphenylphosphonium cation (TPP+) specifically designed to penetrate into the IMM (Murphy & Smith 2007). In mitoQ, TPP^+ is connected to the antioxidant by a 10-carbon alkyl chain (i.e. decyl-TPP^+). The length of this molecule, however, increases membrane permeability, inhibiting the electron transport chain and rising superoxide radical generation (Reily *et al.* 2013; Trnka, Elkalaf & Anděl 2015; Gottwald *et al.* 2018). Consistent with these negative effects, zebra finches only treated with decyl-TPP^+ developed paler bills than controls (Cantarero & Alonso-Alvarez 2017). In contrast, mitoTEMPO does not include that linker group and

bioRxiv preprint doi: https://doi.org/10.1101/2020.01.14.905745; this version posted January 15, 2020. The copyright holder for this preprint (which was not certified by peer review) is the author/funder. All rights reserved. No reuse allowed without permission.

141 the antioxidant role is played by piperidine nitroxide, which recycles ubiquinol (the
142 reduced ubiquinone form) to ubiquinone (Trnka *et al.* 2008). This lowers mitochondrial
143 superoxide radical concentration (Dikalova *et al.* 2010). Moreover, we have recently
144 found that mitoTEMPO is able to increase ketocarotenoid-based feather redness in males
145 from another bird species (the red crossbill; *Loxia curvirostra*; Cantarero *et al.* 2019
146 preprint).

147 Here, we aimed to go further by artificially increasing the level of the most active
148 thyroid hormone (triiodothyronine; T3), testing its impact on both *CYP2J19* expression
149 and redness. Virtually nothing is known about the potential involvement of thyroid
150 hormones in animal carotenoid-based ornaments. However, thyroid hormones control
151 oxygen consumption and have hypermetabolic effects mediated by changes in
152 mitochondria metabolism (Hwang-Bo, Muramatsu & Okumura 1990; Chastel, Lacroix &
153 Kersten 2003; Seifert *et al.* 2008). High blood levels of thyroid hormones are commonly
154 associated with higher oxidative stress, and higher reactive oxygen species (ROS)
155 production, particularly mitochondrial superoxide production (reviewed e.g. in Venditti
156 & Meo 2006; Collin *et al.* 2009; Elnakish *et al.* 2015; Chainy & Sahoo 2019). High
157 oxidative stress may, in turn, exert an inhibitory effect on the activity of CYP enzymatic
158 activity (Zangar, Davydov & Verma 2004). Moreover, high thyroid levels have also been
159 linked to reduced expression of some CYP genes (Honkakoski & Negishi 2000; Kot &
160 Daniel 2011). Accordingly, and also taking into account the precedent results (i.e.
161 Cantarero & Alonso-Alvarez 2017; Cantarero *et al.* 2019 preprint), we hypothesized that
162 mitoTEMPO should increase CYP2J19 activity and bill redness, whereas high T3 levels
163 should decrease them, both treatments interacting perhaps to cancel out their respective
164 effects.
165

bioRxiv preprint doi: https://doi.org/10.1101/2020.01.14.905745; this version posted January 15, 2020. The copyright holder for this preprint (which was not certified by peer review) is the author/funder. All rights reserved. No reuse allowed without permission.

Material and Methods

Experimental protocol

Eighty-six male zebra finches were housed in cages placed within an indoor aviary (more details in Supplementary Material, SM). Two birds were housed per cage (0.6 m × 0.4 m × 0.4 m). The pair was divided by a grille hindering physical contact. After an 8-day acclimation period, all the birds were randomly assigned to the treatments. All of them received a subcutaneous silicone implant (OD 1.96 mm, ID 1.477 mm; Silastic®) empty or filled with T3 (3,3′,5-Triiodo-L-thyronine; SIGMA ref. T2822; see also SM). The T3-filled implants were made at different lengths (6 mm, 8 mm and 10 mm) to produce different dosages. Control birds (n = 22) received a 10 mm empty implant. The largest length was chosen considering recent studies in Gambel's white-crowned sparrows (*Zonotrichia leucophrys gambelii* (Perez *et al.* 2016; 2018). Lower dosages were included considering that sparrows are heavier than finches (26 vs. 15 gr approx., respectively). The implants were put in two consecutive days due to time constraints. Thirty-five birds rejected the implant 2-7 days before the end of the experiment (mean ± SD: 3 ± 1.2 days). The treatment distribution among birds losing or maintaining the implant never differs (i.e. by testing both treatments separately or a single eight-level factor all χ^2 tests: p >0.26). The number of days with implant also did not differ among treatments (non-parametric Kruskal-Wallis or Mann-Whitney U's tests: all p-values >0.30). This variable never produced a significant effect (all p-values > 0.10) when tested as a covariate in every statistical model, and was therefore removed (see below).

Each implant group (Control [C], 6 mm [T3-1], 8 mm [T3-2], 10 mm [T3-3]) was divided by half (9-11 birds per group) to assign the antioxidant treatment (Serum [S] or MitoTEMPO [MT]). This was administered by subcutaneous injections in the skin of the back. MT-treated birds received mitoTEMPO at 1.6 mg/ml in 50 µl saline. S-treated birds

bioRxiv preprint doi: https://doi.org/10.1101/2020.01.14.905745; this version posted January 15, 2020. The copyright holder for this preprint (which was not certified by peer review) is the author/funder. All rights reserved. No reuse allowed without permission.

191 received the same saline volume only. MT-treated birds received 80 µg of mitoTEMPO
192 every other day to a total of seven doses (2.67 mg/Kg/day). First injections were
193 performed two days after the surgery to allow birds' recovery and ended 14 days after.
194 The mitoTEMPO dosage was chosen from results described in mice (Vendrov *et al.*
195 2015), from a precedent pilot study in zebra finches, and also from an experiment in red
196 crossbills (see also SM).

197 Blood samples, digital pictures of the bill, and body mass measures were taken
198 five days before the implant date and again on the last day of the experiment. Blood
199 samples were stored in a cold box and centrifuged 10 min at 12,000 rpm within 8h of
200 sampling. Plasma was stored at -80ºC until analyses. Body condition (i.e. std. residuals
201 of tarsus length on body mass) was similarly distributed among the treatments and its
202 interaction (all χ^2 tests: $p > 0.10$). The treatments were randomly distributed across the
203 aviary (cage rows and columns). Nonetheless, the two birds in each cage belonged to the
204 same antioxidant treatment. The identity of the cage was, anyway, included as a random
205 term in all statistical models to control for pseudo-replication. One bird (T3-1 and
206 mitoTEMPO-treated) died by unknown reasons the day after the start of the experiment
207 and was removed from the dataset.

208 Finally, the occurrence of a body feather moult was visually established at the end
209 of the experiment by the same observer (AC). Birds were classified as engaged or not in
210 moult (49 vs 36%, respectively).

211

212 <u>Thyroid hormone analyses</u>

213 T3 levels were assessed from one plasma aliquot obtained in the last blood sampling
214 event. Hormone values were measured by means of commercial species-independent

bioRxiv preprint doi: https://doi.org/10.1101/2020.01.14.905745; this version posted January 15, 2020. The copyright holder for this preprint (which was not certified by peer review) is the author/funder. All rights reserved. No reuse allowed without permission.

ELISA kits (Arbor Assays, Ann Arbor, MI; ref. K056-H1). The analyses were made twice per sample in three sessions (intra- and inter-assay CVs = 10.2 and 14.8 %, respectively; see also SM).

Respiratory frequency

With the aim of validating the hypermetabolic effect of thyroid hormones (e.g. Harper & Seifert 2008), the respiratory frequency was measured just before each blood sampling event by the same observer (AC). The number of breast movements in 90 seconds was counted by handing each bird face up at the left hand, with the head between the middle and forefinger (Fucikova *et al.* 2009).

Plasma carotenoids

Total carotenoid levels in plasma were determined at the start and end of the experiment by means of spectrophotometry. Samples were diluted in ethanol, centrifuged and supernatant absorbance measured at 450 nm. The concentrations were calculated from a lutein standard curve (full description in SM). This protocol was modified from Hargitai *et al.* (2009).

Gene expression

At the end of the experiment, a small layer of the upper surface of the upper mandible ($1mm^3$ approx.) was taken with a small scalpel. The wound was disinfected and covered with blastoestimulina cream ® (Almirall labs, Spain; composed by *Centella asiatica* extract plus neomycin). All birds fully recovered in less than five weeks. The biopsied tissue was immediately introduced in RNAlater at 1:20 volume approximately and stored frozen (-20ºC) until the analyses. Total RNA was extracted using the RNeasy Mini Kit

bioRxiv preprint doi: https://doi.org/10.1101/2020.01.14.905745; this version posted January 15, 2020. The copyright holder for this preprint (which was not certified by peer review) is the author/funder. All rights reserved. No reuse allowed without permission.

(Qiagen). Residual genomic DNA carry-over was removed using the DNase treatment from the same kit. Complementary DNA (cDNA) was prepared from total RNA (~1 µg) using the GRS cDNA Synthesis Kit (GRiSP). Quantitative real-time PCR reactions were performed on the *CYP2J19* gene (target) on cDNA. Reactions were performed by using iTaq Universal SYBR Green Supermix (Bio-Rad Laboratories) in a CFX96 Touch Real-Time PCR Detection System. β-actin was used as housekeeping (control) gene for normalizing expression levels. Primers for both *CYP2J19* and β-actin were taken from a previous study (i.e. Mundy *et al.* 2016). Mean cycle threshold (Ct) values of both genes were obtained from triplicated measures (both Lessells & Boag 1987' *r* values = 0.99). Expression values of target genes are traditionally corrected to the expression of the control gene using a ΔCt approach, but this assumes that the expression of the control gene is kept constant across conditions. Since our experiment is likely to influence overall homeostasis, and therefore impact control gene expression, we obtained normalized Ct values using the method of Cui *et al.* (2015): normalized value = target_Ct value – (*b* x control_Ct value) where *b* is the regression coefficient of the linear regression of mean *CYP2J19* Ct values on mean β-actin Ct values. This normalization removes biases produced when the housekeeping Ct values correlate to Δ-Ct (i.e. *CYP2J19* Ct minus β-actin Ct; i.e. Cui *et al.* 2015).

Colour measurements

Bill redness was determined by means of digital photography (Nikon® D300; full description in SM). Briefly, each bird was placed laterally and a picture of one side of the head was taken. Digital photographs were standardized and analysed using the recently developed 'SpotEgg' software (Gómez & Liñán-Cembrano 2017), an image-processing tool for automatized analysis of avian colouration that solves the need for linearizing the

bioRxiv preprint doi: https://doi.org/10.1101/2020.01.14.905745; this version posted January 15, 2020. The copyright holder for this preprint (which was not certified by peer review) is the author/funder. All rights reserved. No reuse allowed without permission.

camera's response to subtle changes in light intensity (Stevens *et al.* 2007). The mean red, green and blue (RGB) values measured from the lateral area of the bill (upper and lower mandibles) were used to obtain a hue value from the Foley & van Dam (1982) algorithm (see also Cantarero & Alonso-Alvarez 2017). Repeatability (Lessells & Boag 1987) calculated on a set of digital photographs measured twice ($n = 30$) was $r = 0.99$, $p < 0.001$. Since a low hue means a redder colour, the hue value was reversed (multiplied by -1 and adding 11 to attain positive values) to obtain a "redness" variable (also SM).

Statistical analyses

Generalized linear mixed models (GLMMs) were used to test the treatment effects on the final values of T3, respiratory frequency, body mass difference, gene expression levels and redness as dependent variables in separated models (PROC MIXED in SAS version 9.4 software). The body mass difference (g) was calculated by subtracting the final or intermediate measure (i.e. five days before the end of the experiment) to the initial body mass (i.e. at the start of the experiment). The moult occurrence was tested by a binomial model with logit link function (PROC GLIMMIX in SAS). The hormonal treatment (a four-level factor), the antioxidant treatment (two levels), and the location of the bird into the cage (right vs. left side), as well as their interactions, were all tested in every model (also SM). The cage identity was included as a random factor and was non-significant (all p-values > 0.20), except in the bill redness models ($p < 0.01$). Similarly, the laboratory session in T3 and carotenoid analyses (microplate identity) were included as another random factor in models testing T3 and carotenoid plasma values, respectively, and they were also non-significant (three and four-level factor, respectively; all *p-values* > 0.22). In any event, random factors were maintained in all the models for coherence (see e.g. Bolker *et al.* 2009).

bioRxiv preprint doi: https://doi.org/10.1101/2020.01.14.905745; this version posted January 15, 2020. The copyright holder for this preprint (which was not certified by peer review) is the author/funder. All rights reserved. No reuse allowed without permission.

290 Some covariates were tested. In those models testing the body mass difference,
291 the tarsus length was added to test size-independent variability. Bill brightness was
292 included in the bill redness model to avoid the influence of the total amount (intensity) of
293 light reflected from the measured surface (McGraw 2006). This allows discarding the
294 influence of tissue structure (i.e. not pigmentation) on redness values (McGraw 2006).
295 The bill area used to measure the redness was also tested.

296 The initial value of the dependent variable was additionally included as a covariate
297 to avoid subtle initial biases. In this regard, the initial redness was calculated as the
298 standardized residuals obtained from a model including the random factor cage identity
299 as well as bill brightness and surface as covariates (all significant terms, $p < 0.02$). All
300 the models were explored by backward and forward stepwise procedures, removing or
301 including terms ($p > 0.05$ or $p \leq 0.05$, respectively) to obtain the best fitted one. The
302 lowest AIC criterion also agreed with this procedure. LSD *post hoc*s were used for
303 pairwise comparisons. Plasma T3 and carotenoid values were log-transformed to attain
304 normality. Satterthwaite DFs were used. Least square means ± standard error (LSM ± SE
305 hereon) from mixed models are reported, excepting for moult occurrence were raw
306 proportions are given.

307

308 **Results**

309 Thyroid hormone levels

310 The mitoTEMPO treatment or its interaction with T3 treatment did not report significant
311 effects on plasma T3 values (both removed at $p > 0.78$). The backward procedure led to
312 a non-significant T3 treatment factor (i.e. $F_{3,63.3}=1.50$, $p = 0.184$). Nonetheless, T3-2 and
313 T3-3 showed a trend to significantly higher values of plasma T3 than controls (LSD
314 pairwise comparisons: $p = 0.073$ and 0.059, respectively; Figure 1A). When comparing

bioRxiv preprint doi: https://doi.org/10.1101/2020.01.14.905745; this version posted January 15, 2020. The copyright holder for this preprint (which was not certified by peer review) is the author/funder. All rights reserved. No reuse allowed without permission.

315 controls versus the other birds grouped in a single group, a significant effect was detected
316 ($F_{1,67.3}$=4.07, p =0.048; LSM ± SE: 6.66 ± 1.01 and 9.04 ± 0.60 ng/mL, respectively).
317
318 Respiratory frequency
319 In the model testing respiratory frequency, only the T3 treatment effect remained ($F_{3,70.7}$
320 = 8.64, $p < 0.001$; initial value: $F_{1,74.1}$= 19.09, $p < 0.001$). The LSD tests comparing the
321 control group with each T3 treatment always reported $p < 0.001$ (Figure 1B; other
322 pairwise comparisons $p > 0.62$).
323
324 Moult occurrence
325 The T3 treatment affected the moult ($F_{3,81}$= 7.28, p <0.001) — birds with higher doses
326 being more frequently engaged in moult (5, 55, 85 and 91% respectively, from controls
327 to higher dosages). Pairwise comparisons were always $p < 0.048$, excepting at the two
328 highest levels ($p = 0.598$). No other factor remained in the model (all $p > 0.25$).
329
330 Body mass difference
331 At the intermediate measure, the interaction between both treatments was non-significant
332 ($p = 0.301$). In the best-fitted model, the antioxidant treatment reported a significant effect
333 (Table 1). MitoTEMPO-treated birds lost less mass than controls (LSM± SE: -0.96 ± 0.09
334 and -1.23 ± 0.09 g, respectively). T3 treatment was also a significant factor (Table 1)
335 because birds in any hormone-treated group lost more mass than controls (all
336 comparisons: $p < 0.001$; Figure 2A). The T3-1 vs T3-3 comparison was also significant
337 ($p = 0.027$). When the final body mass was tested, the treatment interaction reported (p =
338 0.085). Only mitoTEMPO-treated birds not exposed to exogenous T3 increased body
339 mass (Figure 2B), with their weight differing from all other groups (all p-values < 0.028).

bioRxiv preprint doi: https://doi.org/10.1101/2020.01.14.905745; this version posted January 15, 2020. The copyright holder for this preprint (which was not certified by peer review) is the author/funder. All rights reserved. No reuse allowed without permission.

340 Serum-only treated birds also differed or tended to significantly differ from birds in T3-
341 2 and T3-3 dosages (p-range: 0.018-0.066; other $p > 0.10$). If the interaction is removed,
342 only the hormone treatment remained ($F_{3,68.2} = 10.58$, $p < 0.001$), controls differing from
343 any other group (all *p-values* < 0.001; other p-values > 0.15; see Table S1 and Figure S1).
344
345 Circulating carotenoids
346 No term reported a significant effect in the model testing plasma carotenoid levels (all p-
347 values > 0.22).
348
349 *CYP2J19* expression
350 The treatments reported a clear highly significant interaction (Table 2). The resulting
351 figure (Figure 3A) resembled that of bill redness at least in the two highest T3 dosages
352 (Figure 3B). MT vs S comparisons at T3-0 (controls), T3-2 and T3-3 hormonal dosages
353 reported $p = 0.035$, 0.032 and 0.055, respectively. A global view suggests a U-shape
354 relationship with hormone dosages among S-injected birds, whereas an inverted U
355 appears among mitoTEMPO-injected animals. Thus, S-injected birds reported lower
356 *CYP2J19* expression at the medium-sized (T3-2) dosage compared to hormone controls
357 ($p = 0.014$; other comparisons among S-injected birds: $p > 0.082$). In mitoTEMPO-
358 treated birds, the control vs T3-2 reported $p = 0.066$, suggesting increased gene expression
359 (Figure 3B). The value then declined at the highest T3 dosage (T3-1 vs T3-3 and T3-2 vs
360 T3-3: both *p-values* < 0.027; other comparisons: p-values > 0.17). It is worth noting that
361 when circulating carotenoids at bill sampling time were added as a covariate, they were
362 positively correlated to gene expression (slope ± SE: 0.059 ± 0.029; $F_{1,72.5} = 4.18$, $p =$
363 0.045), but this did not alter the treatment interaction ($p = 0.013$).
364

bioRxiv preprint doi: https://doi.org/10.1101/2020.01.14.905745; this version posted January 15, 2020. The copyright holder for this preprint (which was not certified by peer review) is the author/funder. All rights reserved. No reuse allowed without permission.

Bill redness

The interaction between both treatments reported a trend to significance ($p = 0.075$; Table 2; also SM for descriptions on other significant terms). This was driven by differences between antioxidant treatments in the two groups with the larger implants (Figure 3A). In serum-injected birds, bill redness increased between T3-2 and T3-3 doses ($p = 0.024$), whereas the opposite pattern was suggested among mitoTEMPO-treated birds (but $p = 0.135$). Moreover, in T3-3-treated individuals, the mitoTEMPO effect showed a trend to significance ($p = 0.062$), here reversing the positive effect of the hormone on redness.

Finally, when *CYP2J19* expression level is included as another covariate in the redness model, the interaction became clearly non-significant ($p = 0.209$), both treatments being subsequently removed (both $p > 0.80$). This covariate then showed a significant positive relationship with redness (i.e. $F_{1,78} = 5.52$, $p = 0.021$; slope ± SE: 0.242 ± 0.103). The regression on raw data was also significant ($r = 0.26$, $p = 0.017$, see Figure 4 and also S3).

Discussion

We have shown that *CYP2J19* expression levels at the bill epidermis positively correlates to the expression of a red carotenoid-based trait and that this link is affected by a mitochondrial antioxidant and a thyroid hormone. T3-treated birds as a single group showed higher hormone levels than controls, as well as higher respiratory frequency and body mass loss, being also engaged in moult. These effects are well-supported by avian literature (Elliott *et al.* 2013; Welcker *et al.* 2013; McNabb & Darras 2015; Perez *et al.* 2018; also SM) and indicate that implants were effective. Moreover, birds with the longest and shortest T3 implants differed in body mass loss, which suggests that the T3 dosage was also relevant. Bill redness and *CYP2J19* expression variability support this view. We

bioRxiv preprint doi: https://doi.org/10.1101/2020.01.14.905745; this version posted January 15, 2020. The copyright holder for this preprint (which was not certified by peer review) is the author/funder. All rights reserved. No reuse allowed without permission.

should, hence, assume that the lack of significant differences in circulating hormone levels among T3-1 to T3-3 groups was probably due to feedback regulation (Leung, Taylor & Van Iderstine 1985; Hull *et al.* 1995; Perez *et al.* 2018), with the effects on target tissues, anyway, differing.

First, we should address the question of why mitoTEMPO-treated birds lost less body mass than other individuals. It contradicts studies where rodents fed with a high caloric diet did not gain mass when treated with this compound (Jeong *et al.* 2016; Gutiérrez-Tenorio *et al.* 2017). Here, mitoTEMPO seems to buffer the body mass loss probably derived from handling stress (see McGraw, Lee & Lewin 2011). In fact, contrarily to typical fatness induced by reduced locomotor activity under captivity, most of our birds lost body mass (Figure 3). Anyway, the addition of body mass change (%) as a covariate to the redness model, even when negatively correlated (birds gaining mass losing redness), did not alter our results (Table S2 and Figure S2). Moreover, this body mass change did not correlate with *CYP2J19* expression (covariate always $p > 0.80$).

In regard to *CYP2J19*, we must first highlight that mitoTEMPO and T3 treatments did not influence circulating carotenoid levels, and the addition of plasma carotenoid values as a covariate to the CYP2J19 model, even when correlated, did not alter the results. Therefore, the experimental effects appear to be, at least partially, independent of changes in substrate availability (yellow carotenoids; McGraw & Toomey 2010). This may support recent ideas suggesting that carotenoid-based signalling is not dependent on resource allocation trade-offs (Koch & Hill 2018) as often defended (e.g. Alonso-Alvarez *et al.* 2008; García-de Blas, Mateo & Alonso-Alvarez 2016).

Moreover, we detected a significant interaction between mitoTEMPO and T3 treatments on *CYP2J19* expression, but the results did not follow our initial predictions (Figure 4). Contrarily to our expectations, mitoTEMPO downregulated *CYP2J19*

bioRxiv preprint doi: https://doi.org/10.1101/2020.01.14.905745; this version posted January 15, 2020. The copyright holder for this preprint (which was not certified by peer review) is the author/funder. All rights reserved. No reuse allowed without permission.

415 expression among hormone controls, although this was not reflected in bill redness
416 variability (see also below). Such a ketolase downregulation apparently contradicts the
417 effects of another mito-targeted molecule (mitoQ) that improved zebra finch bill redness
418 (Cantarero & Alonso-Alvarez 2017). We argue that this is a consequence of subtle
419 differences in the action mechanisms of mitoQ and mitoTEMPO. The first is a synthetic
420 ubiquinone that improves electron transfer at the IMM, whereas mitoTEMPO is a
421 superoxide dismutase (SOD) mimetic that favours ubiquinone recycling by reducing
422 superoxide production (Murphy & Smith 2007; Trnka *et al.* 2008; Dikalova *et al.* 2010).
423 Another difference is the shorther length of the alkyl chain of mitoTEMPO compared to
424 mitoQ. This is likely to have improved the antioxidant action, avoiding disruption of the
425 mitochondrial membrane and higher superoxide production (Reily *et al.* 2013; Trnka,
426 Elkalaf & Anděl 2015; Gottwald *et al.* 2018). In this regard, a comparison of the effects
427 of mitoQ and a very similar compound (mitoTEMPOL) in human cancer cell lines
428 revealed lower levels of superoxide generation in those cells treated with the second
429 compound (Pokrzywinski *et al.* 2016). We thus hypothesize that mitoTEMPO induced a
430 strong reduction in superoxide levels (see Dikalova *et al.* 2010) that could have disrupted
431 cell redox signalling mechanisms linked to ketolase gene expression. We note that
432 superoxide is a well-known redox signal affecting the expression of many genes
433 (reviewed in Hurd & Murphy 2009; Weidinger & Kozlov 2015). In support of this, it has
434 been shown that mitoTEMPO can induce downregulation of human inflammatory and
435 cancer-related genes by interfering redox signalling pathways as a result of a decline in
436 mitochondrial superoxide generation (Nazarewicz *et al.* 2013; McCarthy & Kenny 2016).
437 The inhibitory effect of mitoTEMPO on *CYP2J19* expression also contradicts a
438 recent study where male captive red crossbills treated with the same compound and
439 dosage have regrown redder feathers after plucking (Cantarero *et al.* 2019 preprint).

bioRxiv preprint doi: https://doi.org/10.1101/2020.01.14.905745; this version posted January 15, 2020. The copyright holder for this preprint (which was not certified by peer review) is the author/funder. All rights reserved. No reuse allowed without permission.

Interestingly, in that study, the effect was only detected among the reddest birds at the start of the experiment (supposedly the high-quality animals; Cantarero *et al.* 2019 preprint). This strongly points to other factors controlling mitoTEMPO action on ketolase activity. Perhaps the answer comes from the mitoTEMPO x T3 interaction here showed.

Thus, the mitoTEMPO-induced *CYP2J19* downregulation showed in hormone controls disappeared from T3-1 to T3-2 (Figure 4A). The hormone treatment effect on antioxidant controls, in fact, inhibited *CYP2J19* expression throughout the same dosage range. As previously mentioned, in mammals, but also birds, thyroid hormones have been linked to high ROS generation and oxidative stress (reviewed in Venditti & Meo 2006; Rey *et al.* 2013; Venditti *et al.* 2015) due to increased oxidative metabolism (i.e. oxygen consumption rate) (e. g. Hulbert 2000), and we know that ROS can inhibit CYP levels and activity (see El-Kadi *et al.* 2000 for an example of oxidative stress on P450 activity). The presence of the mito-targeted antioxidant mitoTEMPO at T3-2 dosage reversed the inhibitory effect of T3 and even induced higher ketolase expression compared to hormone controls treated with the antioxidant. Subsequently, at the highest T3 dosage, the birds seem to be able to trigger some compensatory mechanism as *CYP2J19* expression apparently increased (Figure 4A).

Literature from mammalian models supports the capacity of thyroid hormones to mount compensatory/protective responses against its own pro-oxidant effects (e.g. reviewed in Villanueva, Alva-Sánchez & Pacheco-Rosado 2013; Goharbari, Shadboorestan & Abdollahi 2016). For example, in rats, hyperthyroidism leads to increased activity of thioredoxin/peroxiredoxin enzymes transforming hydrogen peroxide (derived from superoxide) to water (Venditti *et al.* 2015). T3 can also upregulate genes involved in mitochondrial biogenesis, thus reducing mitochondrial damage accumulation (Weitzel & Alexander Iwen 2011) or directly upregulating gene expression of different

bioRxiv preprint doi: https://doi.org/10.1101/2020.01.14.905745; this version posted January 15, 2020. The copyright holder for this preprint (which was not certified by peer review) is the author/funder. All rights reserved. No reuse allowed without permission.

p450 enzymes (Brtko & Dvorak 2011; Tee *et al.* 2011). In birds, T3-treated chicken increased SOD activity compared to controls, which apparently avoided oxidative damage (Lin, Decuypere & Buyse 2008). In the same line, T3-treated Muscovy ducklings (*Cairina moschata*) upregulated the gene expression of uncoupling proteins (UCPs) located at the IMM, which are involved in decoupling cell respiration from ATP synthesis allowing a decrease in superoxide generation (e.g. Rey *et al.* 2010). In any event, mitoTEMPO seems to be able to disable that compensatory mechanism (see Figure 4 at T3-3), perhaps by interfering in redox signalling such as suggested for the hormone control group (above).

Although *CYP2J19* expression levels and redness showed the same pattern of change at the two highest T3 dosages (Figure 4), the correlation between both variables is far from perfect (Figure 5). Thus, the mitoTEMPO-induced *CYP2J19* downregulation did not lead to paler bills among hormone controls. This perhaps reveals a delay in the mitoTEMPO effect as colouration could not only depend on the number of ketolase copies but on ketolase activity. Moreover, colouration effects could also have been mediated by post-transcriptional regulation attenuating the impairing effect on colouration (e.g. Smutny, Mani & Pavek 2013). The fact that *CYP2J19* expression and redness variabilities varied in concert at the highest T3 dosages may suggest that the mitoTEMPO impact on the phenotype was quicker under the hypermetabolic effects of the thyroid hormone.

Overall, our results reveal an interacting effect of mitochondrial antioxidant metabolism and thyroid hormones that suggests that certain levels of superoxide are needed to maintain efficient carotenoid biotransformation (see also García-de Blas, Mateo & Alonso-Alvarez 2016). Understanding this mechanism would require future correlational and experimental approaches. This includes determining mitochondrial superoxide production changes as well as variability in ketocarotenoid concentrations at

bioRxiv preprint doi: https://doi.org/10.1101/2020.01.14.905745; this version posted January 15, 2020. The copyright holder for this preprint (which was not certified by peer review) is the author/funder. All rights reserved. No reuse allowed without permission.

the ornament tissue. Nonetheless, this is the first study showing a positive significant correlation between *CYP2J19* expression level and red colouration in any species. Moreover, mitoTEMPO effects give additional support to the hypothesis that the mitochondrion is involved in colour-based sexual signalling (Johnson & Hill 2013; Cantarero & Alonso-Alvarez 2017), also supporting that red ketocarotenoid-based ornaments could act as indices revealing the individual capacity to efficiently perform cell respiration under a sexual selection scenario (Hill 2011; Hill & Johnson 2012). Finally, thyroid effects on avian carotenoid-based colouration have virtually been ignored. We have only been able to find a single study (Schereschewsky 1929), where male bullfinches (*Pyrrhula pyrrhula*) supplied with a thyroid extract moulted paler plumages, which may support some of our findings. Our results thus open a landscape for future studies.

References

Alonso-Alvarez, C., Pérez-Rodríguez, L., Mateo, R., Chastel, O. & Viñuela, J. (2008) The oxidation handicap hypothesis and the carotenoid allocation trade-off. *Journal of Evolutionary Biology,* **21,** 1789-1797.

Biernaskie, J.M., Grafen, A. & Perry, J.C. (2014) The evolution of index signals to avoid the cost of dishonesty. *Proceedings of the Royal Society B: Biological Sciences,* **281,** 20140876.

Bolker, B.M., Brooks, M.E., Clark, C.J., Geange, S.W., Poulsen, J.R., Stevens, M.H.H. & White, J.-S.S. (2009) Generalized linear mixed models: a practical guide for ecology and evolution. *Trends in Ecology & Evolution,* **24,** 127-135.

bioRxiv preprint doi: https://doi.org/10.1101/2020.01.14.905745; this version posted January 15, 2020. The copyright holder for this preprint (which was not certified by peer review) is the author/funder. All rights reserved. No reuse allowed without permission.

513 Britton, G. (2008) Functions of Intact Carotenoids. *Carotenoids: Volume 4: Natural*
514 *Functions* (eds G. Britton, S. Liaaen-Jensen & H. Pfander), pp. 189-212.
515 Birkhäuser Basel, Basel.
516 Brtko, J. & Dvorak, Z. (2011) Role of retinoids, rexinoids and thyroid hormone in the
517 expression of cytochrome p450 enzymes. *Current Drug Metabolism,* **12,** 71-88.
518 Cantarero, A. & Alonso-Alvarez, C. (2017) Mitochondria-targeted molecules determine
519 the redness of the zebra finch bill. *Biology Letters,* **13**.
520 Cantarero, A., Mateo, R., Camarero, P., Alonso, D., Fernandez-Eslava, B. & Alonso-
521 Alvarez, C. (2019) A mitochondria-targeted antioxidant affects the carotenoid-
522 based plumage of red crossbills. *bioRxiv***,** 839670.
523 Collin, A., Joubert, R., Swennen, Q., Damon, M., Coustard, S.M., Skiba-Cassy, S.,
524 Everaert, N., Buyse, J. & Tesseraud, S. (2009) Involvement of thyroid hormones
525 in the regulation of mitochondrial oxidations in mammals and birds. *Thyroid*
526 *Hormones: Functions, Related Diseases and Uses* (eds F.S. Kuehn & M.P.
527 Lozada), pp. 93-107.
528 Cui, X., Yu, S., Tamhane, A., Causey, Z.L., Steg, A., Danila, M.I., Reynolds, R.J., Wang,
529 J., Wanzeck, K.C., Tang, Q., Ledbetter, S.S., Redden, D.T., Johnson, M.R. &
530 Bridges, S.L. (2015) Simple regression for correcting ΔCt bias in RT-qPCR low-
531 density array data normalization. *BMC genomics,* **16,** 82.
532 Chainy, G.B.N. & Sahoo, D.K. (2019) Hormones and oxidative stress: an overview. *Free*
533 *Radical Research***,** 1-26.
534 Chastel, O., Lacroix, A. & Kersten, M. (2003) Pre-breeding energy requirements: thyroid
535 hormone, metabolism and the timing of reproduction in house sparrows *Passer*
536 *domesticus*. *Journal of Avian Biology,* **34,** 298-306.

bioRxiv preprint doi: https://doi.org/10.1101/2020.01.14.905745; this version posted January 15, 2020. The copyright holder for this preprint (which was not certified by peer review) is the author/funder. All rights reserved. No reuse allowed without permission.

537 Dikalova, A.E., Bikineyeva, A.T., Budzyn, K., Nazarewicz, R.R., McCann, L., Lewis,
538 W., Harrison, D.G. & Dikalov, S.I. (2010) Therapeutic targeting of mitochondrial
539 superoxide in hypertension. *Circulation research,* **107,** 106-116.
540 El-Kadi, A.O.S., Bleau, A.-M., Dumont, I., Maurice, H. & du Souich, P. (2000) Role of
541 reactive oxygen intermediates in the decrease of hepatic cytochrome P450 activity
542 by serum of humans and rabbits with an acute inflammatory reaction. *Drug*
543 *Metabolism and Disposition,* **28,** 1112-1120.
544 Elnakish, M.T., Schultz, E.J., Gearinger, R.L., Saad, N.S., Rastogi, N., Ahmed, A.A.E.,
545 Mohler, P.J. & Janssen, P.M.L. (2015) Differential involvement of various
546 sources of reactive oxygen species in thyroxin-induced hemodynamic changes
547 and contractile dysfunction of the heart and diaphragm muscles. *Free Radical*
548 *Biology and Medicine,* **83,** 252-261.
549 Elliott, K.H., Welcker, J., Gaston, A.J., Hatch, S.A., Palace, V., Hare, J.F., Speakman,
550 J.R. & Anderson, W.G. (2013) Thyroid hormones correlate with resting metabolic
551 rate, not daily energy expenditure, in two charadriiform seabirds. *Biology Open,*
552 **2,** 580-586.
553 Foley, J.D. & Van Dam, A. (1982) *Fundamentals of interactive computer graphics*.
554 Addison-Wesley, Reading, MA.
555 Fucikova, E., Drent, P.J., Smits, N. & Van Oers, K. (2009) Handling stress as a
556 measurement of personality in great tit nestlings (*Parus major*). *Ethology,* **115,**
557 366-374.
558 García-de Blas, E., Mateo, R. & Alonso-Alvarez, C. (2016) Specific carotenoid pigments
559 in the diet and a bit of oxidative stress in the recipe for producing red carotenoid-
560 based signals. *PeerJ,* **4,** e2237.

bioRxiv preprint doi: https://doi.org/10.1101/2020.01.14.905745; this version posted January 15, 2020. The copyright holder for this preprint (which was not certified by peer review) is the author/funder. All rights reserved. No reuse allowed without permission.

561 Goharbari, M.H., Shadboorestan, A. & Abdollahi, M. (2016) Inhibitory effects of thyroid
562 hormones on mitochondrial oxidative stress: a systematic review. *International*
563 *Journal of Pharmacology,* **12,** 249-261.
564 Gómez, J. & Liñán-Cembrano, G. (2017) SpotEgg: an image-processing tool for
565 automatised analysis of colouration and spottiness. *Journal of Avian Biology,* **48,**
566 502-512.
567 Gottwald, E.M., Duss, M., Bugarski, M., Haenni, D., Schuh, C.D., Landau, E.M. & Hall,
568 A.M. (2018) The targeted anti-oxidant MitoQ causes mitochondrial swelling and
569 depolarization in kidney tissue. *Physiological Reports,* **6,** e13667.
570 Grafen, A. (1990) Biological signals as handicaps. *Journal of Theoretical Biology,* **144,**
571 517-546.
572 Gutiérrez-Tenorio, J., Marín-Royo, G., Martínez-Martínez, E., Martín, R., Miana, M.,
573 López-Andrés, N., Jurado-López, R., Gallardo, I., Luaces, M., San Román, J.A.,
574 González-Amor, M., Salaices, M., Nieto, M.L. & Cachofeiro, V. (2017) The role
575 of oxidative stress in the crosstalk between leptin and mineralocorticoid receptor
576 in the cardiac fibrosis associated with obesity. *Scientific Reports,* **7,** 16802.
577 Hargitai, R., Arnold, K.E., Herényi, M., Prechl, J. & Török, J. (2009) Egg composition in
578 relation to social environment and maternal physiological condition in the collared
579 flycatcher. *Behavioral Ecology and Sociobiology,* **63,** 869-882.
580 Harper, M.-E. & Seifert, E.L. (2008) Thyroid hormone effects on mitochondrial
581 energetics. *Thyroid,* **18,** 145-156.
582 Hill, G.E. (2011) Condition-dependent traits as signals of the functionality of vital cellular
583 processes. *Ecology Letters,* **14,** 625-634.
584 Hill, G.E., Hood, W.R., Ge, Z., Grinter, R., Greening, C., Johnson, J.D., Park, N.R.,
585 Taylor, H.A., Andreasen, V.A., Powers, M.J., Justyn, N.M., Parry, H.A., Kavazis,

bioRxiv preprint doi: https://doi.org/10.1101/2020.01.14.905745; this version posted January 15, 2020. The copyright holder for this preprint (which was not certified by peer review) is the author/funder. All rights reserved. No reuse allowed without permission.

A.N. & Zhang, Y. (2019) Plumage redness signals mitochondrial function in the house finch. *Proceedings of the Royal Society B: Biological Sciences,* **286,** 20191354.

Hill, G.E. & Johnson, J.D. (2013) The mitonuclear compatibility hypothesis of sexual selection. *Proceedings of the Royal Society B: Biological Sciences,* **280,** 20131314.

Hill, G.E. & Johnson, L.S. (2012) The vitamin A-redox hypothesis: a biochemical basis for honest signaling via carotenoid pigmentation. *American Naturalist,* **180,** E127-150.

Honkakoski, P. & Negishi, M. (2000) Regulation of cytochrome P450 (CYP) genes by nuclear receptors. *Biochem J,* **347,** 321-337.

Hulbert, A.J. (2000) Thyroid hormones and their effects: a new perspective. *Biological Reviews,* **75,** 519-631.

Hull, K.L., Janssens, W.C., Baumbach, W.R. & Harvey, S. (1995) Thyroid glands: novel sites of growth hormone action. *Journal of Endocrinology,* **146,** 449-458.

Hurd, T.R. & Murphy, M. (2009) Biological systems relevant for redox signaling and control. *Redox signaling and regulation in biology and medicine* (eds C. Jacob & P.G. Winyard). Wiley, Weinheim.

Hwang-Bo, J., Muramatsu, T. & Okumura, J. (1990) Relative biopotency of triiodothyronine and of thyroxine for inducing oxygen consumption in young chicks. *Poultry Science,* **69,** 1027-1029.

Jeong, E.-M., Chung, J., Liu, H., Go, Y., Gladstein, S., Farzaneh-Far, A., Lewandowski, E.D. & Dudley, S.C., Jr. (2016) Role of mitochondrial oxidative stress in glucose tolerance, insulin resistance, and cardiac diastolic dysfunction. *Journal of the American Heart Association,* **5,** e003046.

bioRxiv preprint doi: https://doi.org/10.1101/2020.01.14.905745; this version posted January 15, 2020. The copyright holder for this preprint (which was not certified by peer review) is the author/funder. All rights reserved. No reuse allowed without permission.

611 Johnson, J.D. & Hill, G.E. (2013) Is carotenoid ornamentation linked to the inner
612 mitochondria membrane potential? A hypothesis for the maintenance of signal
613 honesty. *Biochimie,* **95,** 436-444.
614 Johnstone, R.A. (1995) Honest advertisement of multiple qualities using multiple signals.
615 *Journal of Theoretical Biology,* **177,** 87-94.
616 Koch, R.E. & Hill, G.E. (2018) Do carotenoid-based ornaments entail resource trade-
617 offs? An evaluation of theory and data. *Functional Ecology,* **32,** 1908-1920.
618 Kot, M. & Daniel, W.A. (2011) Cytochrome P450 is regulated by noradrenergic and
619 serotonergic systems. *Pharmacological Research,* **64,** 371-380.
620 Lessells, C.M. & Boag, P.T. (1987) Unrepeatable repeatabilities: a common mistake. *Auk,*
621 **104,** 116-121.
622 Leung, F.C., Taylor, J.E. & Van Iderstine, A. (1985) Effects of dietary thyroid hormones
623 on growth, plasma T3 and T4, and growth hormone in normal and hypothyroid
624 chickens. *General and Comparative Endocrinology,* **59,** 91-99.
625 Lin, H., Decuypere, E. & Buyse, J. (2008) Effect of thyroid hormones on the redox
626 balance of broiler chickens. *Asian-Australasian Journal of Animal Sciences,* **21**.
627 Lopes, Ricardo J., Johnson, James D., Toomey, Matthew B., Ferreira, Mafalda S.,
628 Araujo, Pedro M., Melo-Ferreira, J., Andersson, L., Hill, Geoffrey E., Corbo,
629 Joseph C. & Carneiro, M. (2016) Genetic basis for red coloration in birds. *Current*
630 *Biology,* **26,** 1427-1434.
631 Maynard Smith, J. & Harper, D. (2003) *Animal signals*. Oxford University Press, Oxford,
632 U.K.
633 McCarthy, Cathal M. & Kenny, Louise C. (2016) Mitochondrial [dys]function; culprit in
634 pre-eclampsia? *Clinical Science,* **130,** 1179-1184.

bioRxiv preprint doi: https://doi.org/10.1101/2020.01.14.905745; this version posted January 15, 2020. The copyright holder for this preprint (which was not certified by peer review) is the author/funder. All rights reserved. No reuse allowed without permission.

635 McGraw, K.J. (2006) *Mechanics of carotenoid-based coloration*. Cambridge: Harvard
636 University Press.
637 McGraw, K.J., Lee, K. & Lewin, A. (2011) The effect of capture-and-handling stress on
638 carotenoid-based beak coloration in zebra finches. *Journal of Comparative*
639 *Physiology A,* **197,** 683-691.
640 McGraw, K.J. & Toomey, M.B. (2010) Carotenoid accumulation in the tissues of zebra
641 finches: predictors of integumentary pigmentation and implications for carotenoid
642 allocation strategies. *Physiological and Biochemical Zoology,* **83,** 97-109.
643 McNabb, F.M.A. & Darras, V.M. (2015) Thyroids. *Sturkie's Avian Physiology (Sixth*
644 *Edition)* (ed. C.G. Scanes), pp. 535-547. Academic Press, San Diego.
645 Mundy, Nicholas I., Stapley, J., Bennison, C., Tucker, R., Twyman, H., Kim, K.-W.,
646 Burke, T., Birkhead, Tim R., Andersson, S. & Slate, J. (2016) Red carotenoid
647 coloration in the zebra finch is controlled by a cytochrome P450 gene cluster.
648 *Current Biology,* **26,** 1435-1440.
649 Murphy, M.P. & Smith, R.A. (2007) Targeting antioxidants to mitochondria by
650 conjugation to lipophilic cations. *Annu Rev Pharmacol Toxicol,* **47,** 629-656.
651 Nazarewicz, R.R., Dikalova, A., Bikineyeva, A., Ivanov, S., Kirilyuk, I.A., Grigor'ev,
652 I.A. & Dikalov, S.I. (2013) Does scavenging of mitochondrial superoxide
653 attenuate cancer prosurvival signaling pathways? *Antioxidants & Redox*
654 *Signaling,* **19,** 344-349.
655 Perez, J.H., Furlow, J.D., Wingfield, J.C. & Ramenofsky, M. (2016) Regulation of vernal
656 migration in Gambel's white-crowned sparrows: Role of thyroxine and
657 triiodothyronine. *Hormones and Behavior,* **84,** 50-56.
658 Perez, J.H., Meddle, S.L., Wingfield, J.C. & Ramenofsky, M. (2018) Effects of thyroid
659 hormone manipulation on pre-nuptial molt, luteinizing hormone and testicular

bioRxiv preprint doi: https://doi.org/10.1101/2020.01.14.905745; this version posted January 15, 2020. The copyright holder for this preprint (which was not certified by peer review) is the author/funder. All rights reserved. No reuse allowed without permission.

growth in male white-crowned sparrows (*Zonotrichia leuchophrys gambelii*). *General and Comparative Endocrinology,* **255,** 12-18.

Pokrzywinski, K.L., Biel, T.G., Kryndushkin, D. & Rao, V.A. (2016) Therapeutic targeting of the mitochondria initiates excessive superoxide production and mitochondrial depolarization causing decreased mtDNA integrity. *Plos One,* **11,** e0168283.

Reby, D. & McComb, K. (2003) Anatomical constraints generate honesty: acoustic cues to age and weight in the roars of red deer stags. *Animal Behaviour,* **65,** 519-530.

Reily, C., Mitchell, T., Chacko, B.K., Benavides, G.A., Murphy, M.P. & Darley-Usmar, V.M. (2013) Mitochondrially targeted compounds and their impact on cellular bioenergetics. *Redox Biology,* **1,** 86-93.

Rey, B., Roussel, D., Romestaing, C., Belouze, M., Rouanet, J.L., Desplanches, D., Sibille, B., Servais, S. & Duchamp, C. (2010) Up-regulation of avian uncoupling protein in cold-acclimated and hyperthyroid ducklings prevents reactive oxygen species production by skeletal muscle mitochondria. *BMC Physiol,* **10,** 5.

Rey, B., Roussel, D., Rouanet, J.-L. & Duchamp, C. (2013) Differential effects of thyroid status on regional H_2O_2 production in slow- and fast-twitch muscle of ducklings. *Journal of Comparative Physiology B,* **183,** 135-143.

Schereschewsky, H. (1929) Einige Beiträge zum Problem der Verfärbung des Gefieders beim Gimpel. *Wilhelm Roux Arch Entwickl Mech Org,* **115,** 110-153.

Seifert, E.L., Bézaire, V., Estey, C. & Harper, M.-E. (2008) Essential role for uncoupling protein-3 in mitochondrial adaptation to fasting but not in fatty acid oxidation or fatty acid anion export. *Journal of Biological Chemistry,* **283,** 25124-25131.

bioRxiv preprint doi: https://doi.org/10.1101/2020.01.14.905745; this version posted January 15, 2020. The copyright holder for this preprint (which was not certified by peer review) is the author/funder. All rights reserved. No reuse allowed without permission.

683 Smith, R.A.J., Porteous, C.M., Gane, A.M. & Murphy, M.P. (2003) Delivery of bioactive
684 molecules to mitochondria in vivo. *Proceedings of the National Academy of*
685 *Sciences of the United States of America,* **100,** 5407-5412.
686 Smutny, T., Mani, S. & Pavek, P. (2013) Post-translational and post-transcriptional
687 modifications of pregnane x receptor (pxr) in regulation of the cytochrome p450
688 superfamily. *Current Drug Metabolism,* **14,** 1059-1069.
689 Stevens, M., Párraga, C.A., Cuthill, I.C., Partridge, J.C. & Troscianko, T.S. (2007) Using
690 digital photography to study animal coloration. *Biological Journal of the Linnean*
691 *Society,* **90,** 211-237.
692 Stradi, R., Celentano, G., Boles, M. & Mercato, F. (1997) Carotenoids in bird plumage:
693 the pattern in a series of red-pigmented *Carduelinae*. *Comparative Biochemistry*
694 *and Physiology Part B: Biochemistry and Molecular Biology,* **117,** 85-91.
695 Tee, M.K., Huang, N., Damm, I. & Miller, W.L. (2011) Transcriptional regulation of the
696 human p450 oxidoreductase gene: hormonal regulation and influence of promoter
697 polymorphisms. *Molecular Endocrinology,* **25,** 715-731.
698 Tompkins, L.M. & Wallace, A.D. (2007) Mechanisms of cytochrome P450 induction.
699 *Journal of Biochemical and Molecular Toxicology,* **21,** 176-181.
700 Trnka, J., Blaikie, F.H., Smith, R.A.J. & Murphy, M.P. (2008) A mitochondria-targeted
701 nitroxide is reduced to its hydroxylamine by ubiquinol in mitochondria. *Free*
702 *Radical Biology and Medicine,* **44,** 1406-1419.
703 Trnka, J., Elkalaf, M. & Anděl, M. (2015) Lipophilic triphenylphosphonium cations
704 inhibit mitochondrial electron transport chain and induce mitochondrial proton
705 leak. *Plos One,* **10,** e0121837.

bioRxiv preprint doi: https://doi.org/10.1101/2020.01.14.905745; this version posted January 15, 2020. The copyright holder for this preprint (which was not certified by peer review) is the author/funder. All rights reserved. No reuse allowed without permission.

706 Twyman, H., Prager, M., Mundy, N.I. & Andersson, S. (2018) Expression of a
707 carotenoid-modifying gene and evolution of red coloration in weaverbirds
708 (*Ploceidae*). *Molecular Ecology,* **27,** 449-458.
709 Twyman, H., Valenzuela, N., Literman, R., Andersson, S. & Mundy, N.I. (2016) Seeing
710 red to being red: conserved genetic mechanism for red cone oil droplets and co-
711 option for red coloration in birds and turtles. *Proceedings of the Royal Society B:*
712 *Biological Sciences,* **283,** 20161208.
713 Vanhooydonck, B., van Damme, R., Herrel, A. & Irschick, D.J. (2007) A performance
714 based approach to distinguish indices from handicaps in sexual selection studies.
715 *Functional Ecology,* **21,** 645-652.
716 Venditti, P. & Meo, S.D. (2006) Thyroid hormone-induced oxidative stress. *Cellular and*
717 *Molecular Life Sciences CMLS,* **63,** 414-434.
718 Venditti, P., Napolitano, G., Barone, D., Coppola, I. & Di Meo, S. (2015) Effect of thyroid
719 state on enzymatic and non-enzymatic processes in H2O2 removal by liver
720 mitochondria of male rats. *Molecular and Cellular Endocrinology,* **403,** 57-63.
721 Vendrov, A.E., Vendrov, K.C., Smith, A., Yuan, J., Sumida, A., Robidoux, J., Runge,
722 M.S. & Madamanchi, N.R. (2015) NOX4 NADPH oxidase-dependent
723 mitochondrial oxidative stress in aging-associated cardiovascular disease.
724 *Antioxidants & Redox Signaling,* **23,** 1389-1409.
725 Villanueva, I., Alva-Sánchez, C. & Pacheco-Rosado, J. (2013) The role of thyroid
726 hormones as inductors of oxidative stress and neurodegeneration. *Oxidative*
727 *Medicine and Cellular Longevity,* **2013,** 15.
728 Weaver, R.J., Koch, R.E. & Hill, G.E. (2017) What maintains signal honesty in animal
729 colour displays used in mate choice? *Philosophical Transactions of the Royal*
730 *Society B: Biological Sciences,* **372**.

bioRxiv preprint doi: https://doi.org/10.1101/2020.01.14.905745; this version posted January 15, 2020. The copyright holder for this preprint (which was not certified by peer review) is the author/funder. All rights reserved. No reuse allowed without permission.

731 Weidinger, A. & Kozlov, A.V. (2015) Biological activities of reactive oxygen and
732 nitrogen species: oxidative stress versus signal transduction. *Biomolecules,* **5,**
733 472-484.
734 Weitzel, J.M. & Alexander Iwen, K. (2011) Coordination of mitochondrial biogenesis by
735 thyroid hormone. *Molecular and Cellular Endocrinology,* **342,** 1-7.
736 Welcker, J., Chastel, O., Gabrielsen, G.W., Guillaumin, J., Kitaysky, A.S., Speakman,
737 J.R., Tremblay, Y. & Bech, C. (2013) Thyroid hormones correlate with basal
738 metabolic rate but not field metabolic rate in a wild bird species. *Plos One,* **8,**
739 e56229.
740 Zangar, R.C., Davydov, D.R. & Verma, S. (2004) Mechanisms that regulate production
741 of reactive oxygen species by cytochrome P450. *Toxicology and Applied*
742 *Pharmacology,* **199,** 316-331.

bioRxiv preprint doi: https://doi.org/10.1101/2020.01.14.905745; this version posted January 15, 2020. The copyright holder for this preprint (which was not certified by peer review) is the author/funder. All rights reserved. No reuse allowed without permission.

743 **Figure 1.** Plasma T3 levels (A) and respiratory frequency (B) at the end of the experiment
744 depending on the length of the implant filled with T3 (T3-1: 6 mm, T3-2: 8 mm and T3-
745 3: 12 mm). LSM ± SEs from the mixed model.

746

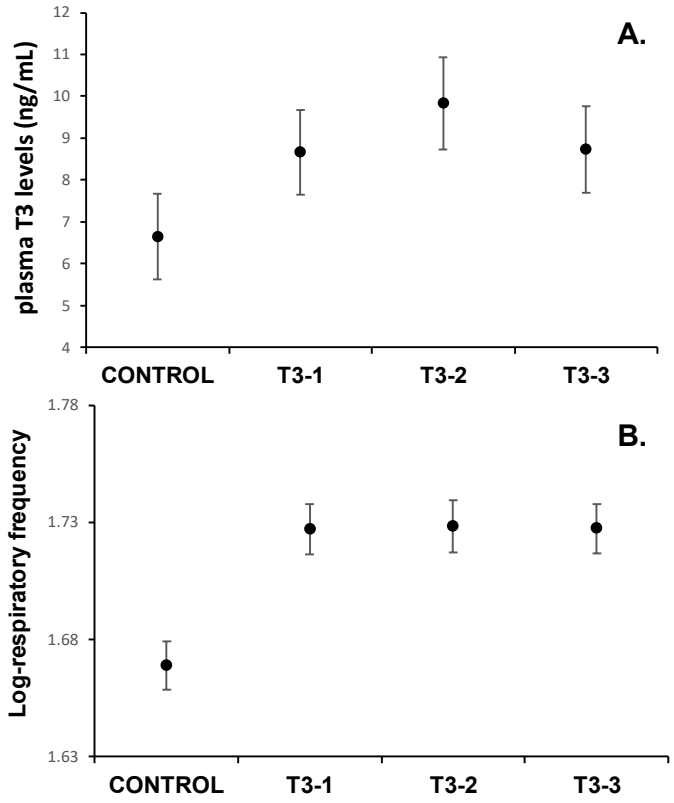

747

748

749

bioRxiv preprint doi: https://doi.org/10.1101/2020.01.14.905745; this version posted January 15, 2020. The copyright holder for this preprint (which was not certified by peer review) is the author/funder. All rights reserved. No reuse allowed without permission.

750 **Figure 2.** Difference between intermediate (A) and final (B) body masses regard to initial
751 pre-experimental values depending on T3 dosage (T3-1: 6mm, T3-2: 8mm and T3-3:
752 12mm) and antioxidant treatment (S: serum; MT: mitoTEMPO). LSM ± SEs from mixed
753 models controlling for body size (tarsus length) variability.
754

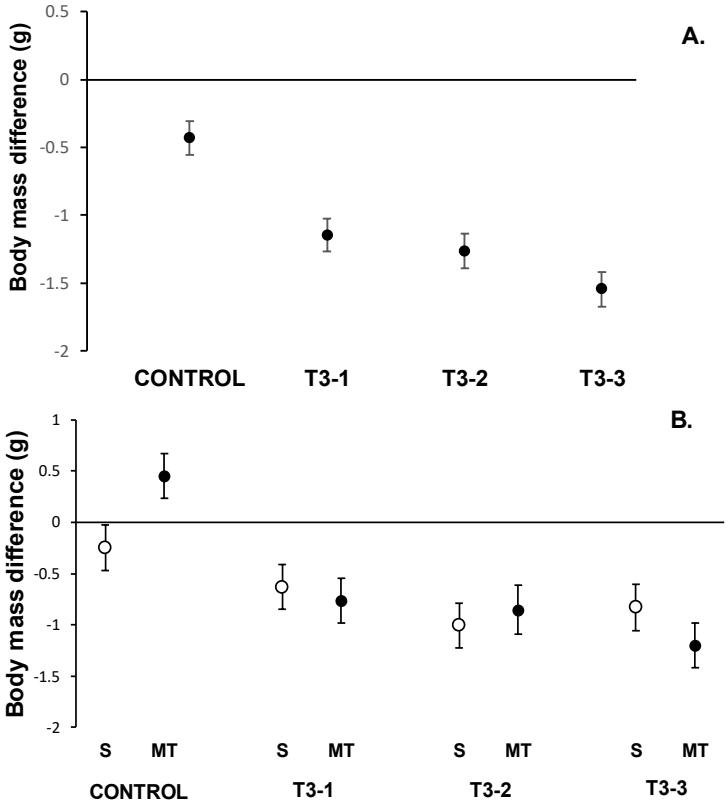

755
756

bioRxiv preprint doi: https://doi.org/10.1101/2020.01.14.905745; this version posted January 15, 2020. The copyright holder for this preprint (which was not certified by peer review) is the author/funder. All rights reserved. No reuse allowed without permission.

757 **Figure 3.** Treatment effects on the *CYP2J19* expression level (A) and bill redness (B).
758 See the description of variables in Methods. (S: serum only; MT: MitoTEMPO-injected
759 birds: T3-1: 6mm, T3-2: 8mm and T3-3: 12mm). LSM ± SE from mixed models.
760

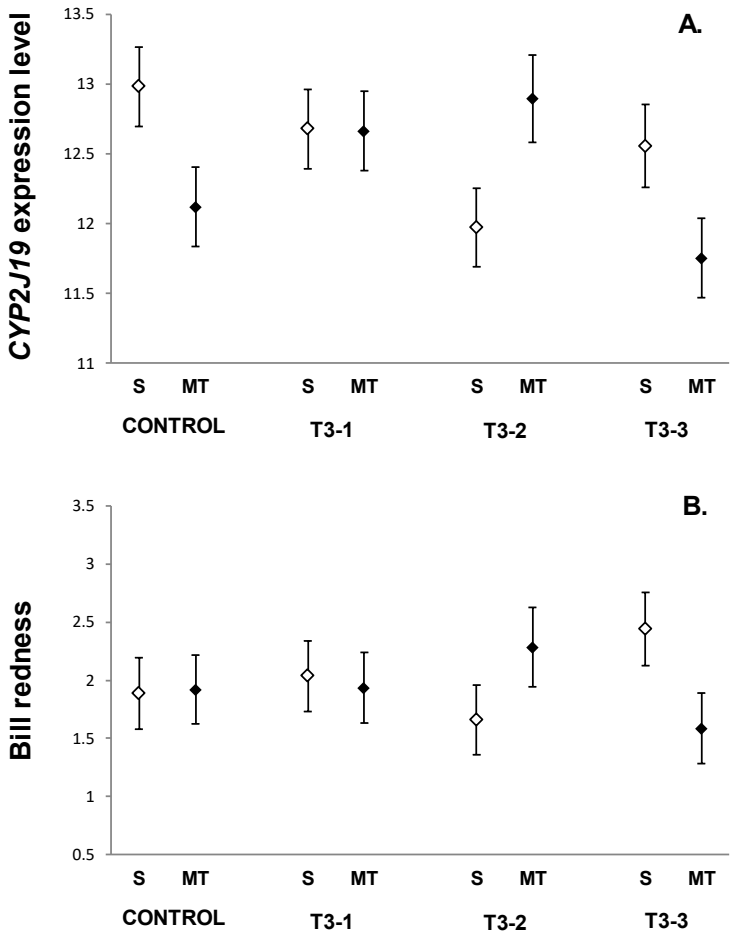

761
762

bioRxiv preprint doi: https://doi.org/10.1101/2020.01.14.905745; this version posted January 15, 2020. The copyright holder for this preprint (which was not certified by peer review) is the author/funder. All rights reserved. No reuse allowed without permission.

763 **Figure 4.** Relationship between male zebra finch bill redness and the expression level of
764 the candidate enzyme for ketocarotenoid synthesis in that ornament (slope ± SD: 0.310 ±
765 0.127). Raw data with redness as the reversed hue value (see Methods).

766

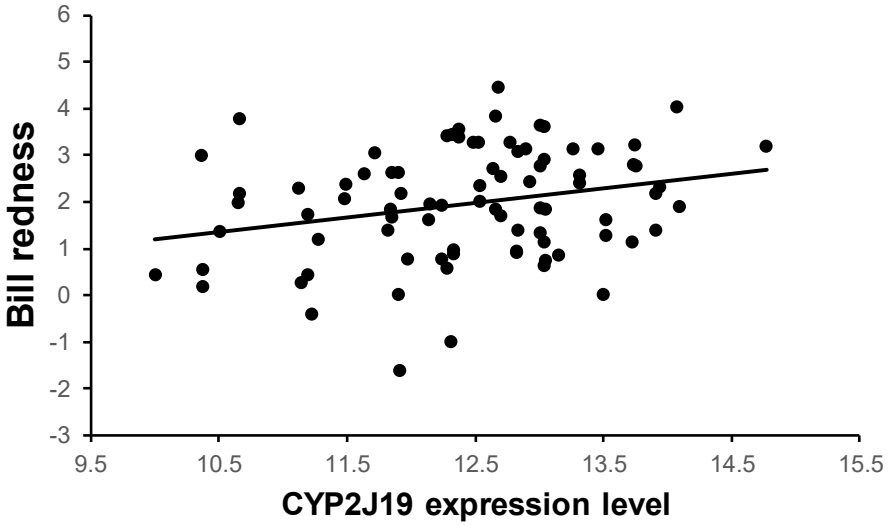

767

bioRxiv preprint doi: https://doi.org/10.1101/2020.01.14.905745; this version posted January 15, 2020. The copyright holder for this preprint (which was not certified by peer review) is the author/funder. All rights reserved. No reuse allowed without permission.

768 **Table 1.** Best fitted models testing body mass variability at two different sampling times
769 (intermediate and final, see main text).
770
771

Intermediate body mass	**Slope ± SE**	***F***	**df**	***p***
MitoTEMPO treatment	-	4.38	1,41	0.043
T3 treatment	-	15.09	3,65.7	< 0.001
Initial body mass	-0.175 ± 0.043	16.52	1,76.9	< 0.001
Tarsus length	0.244 ± 0.116	4.45	1,74.6	0.038

776

Final body mass	**Slope ± SE**	***F***	**df**	***p***
MitoTEMPO treatment	-	39.5	0.29	0.595
T3 treatment	-	65.3	2.30	0.085
Initial body mass	-0.173 ± 0.054	73.9	10.13	0.002
Tarsus length	0.430 ± 0.149	71.3	8.35	0.005

782

bioRxiv preprint doi: https://doi.org/10.1101/2020.01.14.905745; this version posted January 15, 2020. The copyright holder for this preprint (which was not certified by peer review) is the author/funder. All rights reserved. No reuse allowed without permission.

783 **Table 2.** Best fitted models testing the impact of the mitoTEMPO and T3 treatments on
784 male zebra finch bill *CYP2J19* expression and redness.
785

CYP2J19	**Slope ± SE**	***F***	**df**	***p***
MitoTEMPO treatment	-	0.71	1,42.2	0.405
T3 treatment	-	1.20	3,65.6	0.318
MitoTEMPO x T3 treatments	-	4.15	3,67.5	0.009
Bill redness	**Slope ± SE**	***F***	**df**	***p***
MitoTEMPO treatment	-	0.08	1,38.7	0.777
T3 treatment	-	0.08	3,53.3	0.973
MitoTEMPO x T3 treatments	-	2.42	3,58.6	0.075
Location into the cage	-	9.49	1,29.4	0.004
Measured area (mm^2)	0.055 ± 0.027	4.22	1,50.6	0.045
Initial bill redness (residuals)	0.355 ± 0.161	4.85	1,37.5	0.034
Bill brightness	-6.919 ± 1.007	47.18	1,55.8	<.0001

786

Supplementary Material

Additional methodological details

The birds were housed at the Fundación para la Investigación en Etología y Biodiversidad (http://es.fiebfoundation.org). All birds were given *ad libitum* access to food (commercial pelleted food; KIKI®, Spain), water and grit. The temperature (mean ± range 22° ± 1°C) and light daily cycle (16L : 8D) were controlled.

A small incision with a scalpel was made in the skin of birds to introduce the implants, and surgical glue (Cicastick®) of veterinary use was used to close the wounds, though suture (two 17-70 cm stitches of Braun®, Model Novosyn Violet, 6/0 HR) was additionally used.

The mitoTEMPO dosage was chosen from a pilot study involving 10 male zebra finches randomly assigned to different concentrations (0, 0.334, 0.668, 1.335 and 2.67 mg/Kg/day) subcutaneously injected in 50 µl saline every other day for two weeks. The highest level (2.67 mg/Kg/day; 3mM) was chosen as we did not find a significant correlation between dose and body mass change (%; Spearman's $r = 0.320$, $p = 0.367$), suggesting no health impairment. Moreover, no evident toxicity symptoms (behaviour changes, fatigue, lack of alertness) were detected and the change (%) in bill redness increased with dosage (Spearman's $r = 0.82$, $p = 0.01$; see also Cantarero & Alonso-Alvarez 2017 for colour analysis methods)(Cantarero & Alonso-Alvarez 2017). The final dosage was, nonetheless, higher than that reported in mice (1.5 mg/Kg/day; Vendrov *et al.* 2015) where mitoTEMPO decreased mitochondrial free radical production. In the cited study, however, the antioxidant was daily administered for 84 days (here 14 days).

The origin of the birds (three commercial suppliers and one experimental population [i.e. IREC-CSIC; Ciudad Real, Spain]) was also balanced among antioxidant treatments (χ^2=2.73, df=3, $p = 0.435$), T3 implant size (χ^2= 3.86, df = 9, $p = 0.920$) and among the eight combinations (antioxidant x hormone groups: χ^2= 10.81, df = 21, $p = 0.966$).

Implant rejection events

The explanation to implant rejection experienced by some birds was unclear. Although we initially suspected that it could have been due to the implant sealing method, trials with different alternatives (glues or suturing the silicone tube ends) had similar rejection rates. The same Silastic® (Dow Corning) implant type has been used in avian endocrinology studies for decades (Wingfield 1984 and many articles from that researcher; see recently e.g. Noguera, Kim & Velando 2017). We suspect that silicone composition has recently subtly changed as the patented product is currently manufactured by another company (Freudenberg Medical), and we must consider that it was designed for humans/rodent models. In any event, the lack of effect of the "days with implants" covariate and also the randomized distribution of treatments among those birds losing implants suggests that the impact of implant rejection on main conclusions is likely to have been minor.

Hormone analyses

Plasma aliquots were allowed to defrost and equilibrate for an hour at room temperature. A volume of 30 µl of plasma was transferred to labelled glass tubes. Hormone extraction was made by adding 3 ml of diethyl ether to the tubes, vortexing for 5 min and then centrifuging (5 min at 1500 rpm) in at 4ºC. These tubes were maintained in a freezing bath of ethanol plus dry ice for 2 min. The etheric phase was transferred to a new clean tube, which was left to dry out in a warm bath under a fume hood (30 min at 40ºC). This extraction protocol was performed twice. Extractions were re-suspended with 130 µl of steroid buffer (Arbor Assays, Ann Arbor, MI; ref. K056-H1) and vigorously vortexed for 5 min.

The measurements were performed by means of commercial ELISA kits (Arbor Assays, Ann Arbor, MI; ref. K056-H1). A microplate reader was used (Multi-detection Synergy HT; Biotek®). The standard curves provided a very good fit to standards ($r^2 > 0.99$). The detection limit of the assay (80% maximum binding) was found at 0.078 ng/ml. The assays were made twice per sample (intra- and inter-assay CVs = 10.2 and 14.8 % respectively). The recoveries (%) described in another avian study using a similar ELISA kit ranged 93-113% (Elarabany, Abdallah & Said 2012). The analyses were made following the advice of Arbor Assays technicians.

Plasma T3 values in our control and T3-treated birds (mean ± SD, range: 6.64 ± 2.68, 3.83-15.05 and 9.04 ± 5.27, 2.48-29.02, respectively) where within the range reported for this species in other studies (Eng, Williams & Elliott 2013; Yamaguchi *et al.* 2017).

Respiratory frequency

The number of breast movements in 90 seconds was counted by handing the birds face up at the left hand, with the head between the middle and forefinger. Breast movements were registered for 90 s divided into two 45 s bouts. In between these two bouts, the birds were introduced in a fabric bag while its cage mate was captured and its first bout of respiratory frequency measurement was taken (i.e. 2 min approx.). The two 45 s measurements taken to calculate the respiratory frequency value at both the beginning and end of the experiment were highly repeatable (Lessells & Boag 1987)(Lessells & Boag 1987; initial value: $r = 0.93$, final value: $r = 0.97$, both $p < 0.001$). After the measurement, the birds were weighed and bleed.

Plasma carotenoid quantification

Plasma aliquots were allowed to defrost for 20 min at room temperature. 10 µl were transferred to labelled plastic tubes containing 90µl of absolute ethanol, being then vortexed (3 min) and centrifuged (5 min at 11000g) in a cooled centrifuge (4ºC) to precipitate flocculent proteins. The absorbance of the supernatant was measured at the lutein peak (450 nm) by spectrophotometric analyses, using a seven-level calibration curve obtained from serial dilution derived from a tube containing 22.5 µg of lutein in 1500 µL absolute ethanol. The protocol was modified from Hargitai et al. (2009).

Digital photography

For each photo, the same standard grey reference and scale (ColorChecker Classic target; X-Rite, Michigan) was placed next to the bird's head. The focus and diaphragm of the camera were manually fixed to avoid the interference of automatic functions. We have previously

shown that these picture-based measurements are highly correlated with the redness measurement (i.e., red hue) obtained from portable spectrophotometers (Mougeot *et al.* 2007; Alonso-Alvarez & Galván 2011). SpotEgg software, however, allows the user to manually draw any region and provide information about its colouration, shape or other features. The measure of a large delimited area, as opposed to portable spectrophotometers that analyse colouration of reduced spots (usually 1-2 mm), makes this tool useful for evolutionary biologists aiming to capture most of the variability among individuals (Gómez & Liñán-Cembrano 2017). Accordingly, for each animal, the average of red, green, and blue (RGB) components of the lateral bill surface (upper and lower mandibles) were calculated. We used the lateral side of the bill due to the low variance of colouration at the top. We then determined hue values by means of the Foley & van Dam algorithm (1982) (see also main text).

Additional analyses

In the model testing the difference between final and initial size-corrected body mass, the backward procedure at $p < 0.05$ reported that only the hormone treatment factor was retained (Table S1 and Figure S1).

Table S1. Mixed model testing the body mass difference between final and initial measures controlled for body size (tarsus length) and also initial body mass.

Final body mass difference	slope± SE	*F*	df	*P*
T3 treatment	-	10.58	3,68.2	< 0.001
Initial body mass	-0.155 ± 0.055	8.13	1.78.8	0.006
Tarsus length	0.352 ± 0.149	5.66	1.77	0.020

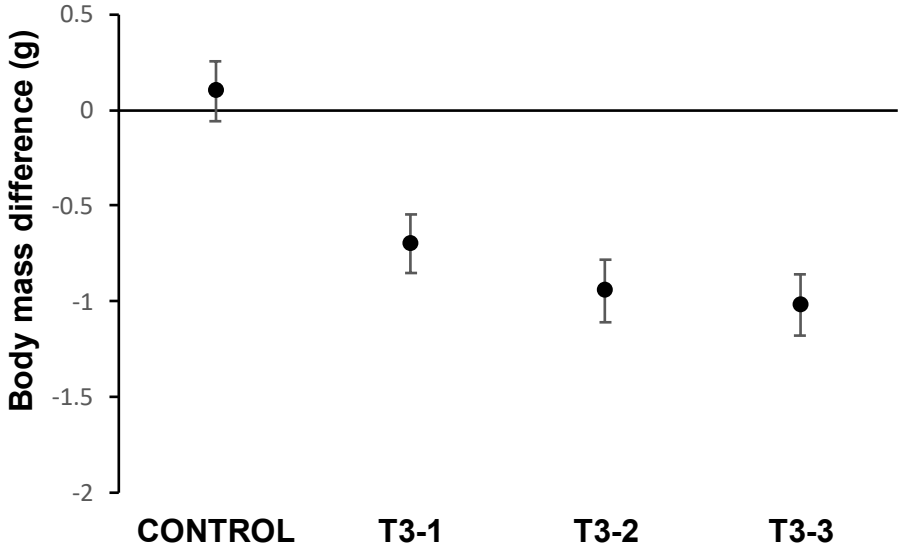

Figure S1. Body mass difference between final and initial measurement depending on T3 dosage (T3-1: 6mm, T3-2: 8mm and T3-3: 12mm). LSM ± SEs from mixed models.

In the model testing final bill redness, when we added body mass change during the experiment (% from initial to final measure) in order to assess hormonal effects independently of T3-mediated body mass effects, the interaction becomes significant (Table S1 and Figure S1). Here, the antioxidant effect at the highest T3 dosage is clearer ($p = 0.032$; LSM ± S.E.: mitoTEMPO: 0.424 ± 0.304; serum: 1.386 ± 0.310). The difference between the two highest T3 dose groups was again evident among antioxidant controls ($p = 0.01$; LSM ± S.E.: 0.550 ± 0.297 and 1.386 ± 0.310, for T3-2 and T3-3, respectively). Among those treated with mitoTEMPO, the T3-2 vs T3-3 comparison reported a p-value = 0.079 (LSM ± S.E.: 1.228 ± 0.332 and 0.424 ± 0.304, for T3-2 and T3-3, respectively), thus suggesting that birds became paler at the highest dose.

Table S2. Model testing the impact of mitoTEMPO and T3 treatments on male bill redness when controlling for body mass change (%; bold) and other factor and covariates.

	Slope ± S.E.	*F*	df	*p*
mitoTEMPO treatment	-	0.05	1, 40.2	0.828
T3 treatment	-	0.22	3, 55.5	0.885
MitoTEMPO x T3 treatments	-	3.40	3, 56.8	0.024
Cage side	-	7.56	1, 30.2	0.010
Measurement area	0.058 ± 0.026	5.18	1, 47.7	0.027
Initial Redness (residuals)	0.276 ± 0.153	3.25	1, 36.2	0.0797
Final bill brightness	-6.999 ± 0.958	53.39	1, 52.4	<.0001
Body mass change (%)	**-0.042 ± 0.017**	**6.08**	**1, 48.6**	**0.017**

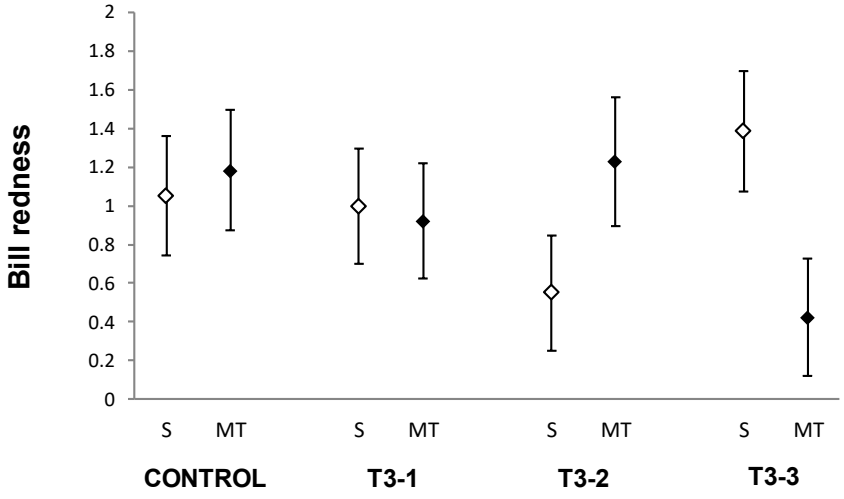

Figure S2. Treatment effects on the bill redness. Bill redness was the result of reversing the hue value (x -1) making data positive by adding a fixed value of 11 (see main text; S: serum only; MT: MitoTEMPO-injected birds: T3-1: 6mm, T3-2: 8mm and T3-3: 12mm). LSM ± SE from mixed models controlling for body mass change (%) during the experiment (see Results).

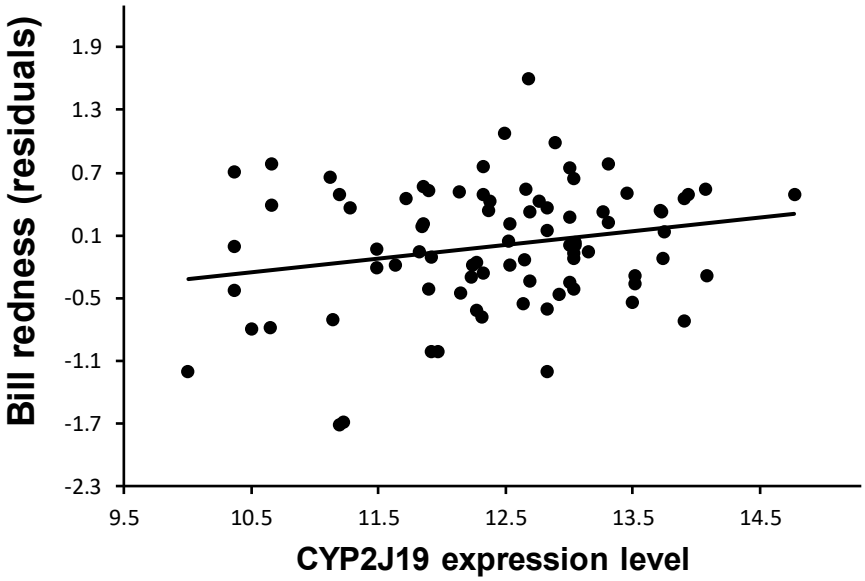

Figure S3. The relationship between bill redness and CYP2J19 expression level. The redness level is here controlled for any other term in the redness model (bill area, brightness, side of the cage and cage identity random factor). See Results section in the main text for the slope ± SE and other details.

Other significant terms in the redness model

In the model testing bill redness (Table 2 in the main text), the location into the cage affected the dependent variable. The bill of those birds placed at the left side was redder than the bill of birds at the right side (LSM ± S.E.: 1.239 ± 0.157 and 0.699 ± 0.157, respectively). This could perhaps be interpreted as birds in the right side being subtly exposed to higher stress levels inhibiting red colouration production. In this regard, we must note that maintenance work daily made (water and food supply) was always made from the left to the right side of the cage. This may have exposed to birds placed in the right side to higher disturbance as both cage sides were only separated by a grille, the bird on the right side enduring more time of disturbance. This apparently subtle influence did only induce a significant effect in the case of the redness model.

159 Regarding other significant terms in the same model (Table 2 in the main text), the
160 bill area was positively related to redness, i.e. larger bills were redder. We have not found a
161 reasonable technical explanation to this effect, though it could be related to individual quality.

162 The initial bill redness, as well as bill brightness at the sampling time, were positively
163 and negatively, respectively, related to final bill redness (Table 2 in the main text). This
164 would, respectively, mean that bill redness was individually repeatable and paler bills
165 reflected more light.

166

167 **References**

168 Alonso-Alvarez, C. & Galván, I. (2011) Free radical exposure creates paler carotenoid-based
169 ornaments - a possible interaction in the expression of black and red traits. *Plos One,* **6,**
170 e19403.

171 Cantarero, A. & Alonso-Alvarez, C. (2017) Mitochondria-targeted molecules determine the redness
172 of the zebra finch bill. *Biology Letters,* **13**.

173 Elarabany, N.F., Abdallah, G.A. & Said, A.E. (2012) Seasonal variations of steroid hormones and
174 triiodothyronine concentrations in migratory northern shovelers. *Journal of Experimental*
175 *Zoology Part A: Ecological Genetics and Physiology,* **317,** 216-226.

176 Eng, M.L., Williams, T.D. & Elliott, J.E. (2013) Developmental exposure to a brominated flame
177 retardant: An assessment of effects on physiology, growth, and reproduction in a songbird,
178 the zebra finch. *Environmental Pollution,* **178,** 343-349.

179 Foley, J.D. & Van Dam, A. (1982) *Fundamentals of interactive computer graphics*. Addison-Wesley,
180 Reading, MA.

181 Gómez, J. & Liñán-Cembrano, G. (2017) SpotEgg: an image-processing tool for automatised analysis
182 of colouration and spottiness. *Journal of Avian Biology,* **48,** 502-512.

183 Hargitai, R., Arnold, K.E., Herényi, M., Prechl, J. & Török, J. (2009) Egg composition in relation to
184 social environment and maternal physiological condition in the collared flycatcher.
185 *Behavioral Ecology and Sociobiology,* **63,** 869-882.

186 Lessells, C.M. & Boag, P.T. (1987) Unrepeatable repeatabilities: a common mistake. *Auk,* **104,** 116-
187 121.

188 Mougeot, F., Pérez-Rodríguez, L., Martínez-Padilla, J., Leckie, F. & Redpath, S.M. (2007) Parasites,
189 testosterone and honest carotenoid-based signalling of health. *Functional Ecology,* **21,** 886-
190 898.

191 Noguera, J.C., Kim, S.Y. & Velando, A. (2017) Family-transmitted stress in a wild bird. *Proceedings*
192 *of the National Academy of Sciences,* **114,** 6794-6799.
193 Vendrov, A.E., Vendrov, K.C., Smith, A., Yuan, J., Sumida, A., Robidoux, J., Runge, M.S. &
194 Madamanchi, N.R. (2015) NOX4 NADPH oxidase-dependent mitochondrial oxidative stress
195 in aging-associated cardiovascular disease. *Antioxidants & Redox Signaling,* **23,** 1389-1409.
196 Wingfield, J.C. (1984) Environmental and endocrine control of reproduction in the song sparrow,
197 *Melospiza melodia*. II. Agonistic interactions as environmental information stimulating
198 secretion of testosterone. *General and Comparative Endocrinology,* **56,** 417-424.
199 Yamaguchi, S., Hayase, S., Aoki, N., Takehara, A., Ishigohoka, J., Matsushima, T., Wada, K. &
200 Homma, K.J. (2017) Sex differences in brain thyroid hormone levels during early post-
201 hatching development in zebra finch (*Taeniopygia guttata*). *Plos One,* **12,** e0169643.